RSC Advances

PAPER

View Article Online
View Journal | View Issue

Cite this: *RSC Adv.*, 2015, **5**, 65560

A new electrochemical sensor based on a nitrogen-doped graphene/$CuCo_2O_4$ nanocomposite for simultaneous determination of dopamine, melatonin and tryptophan

F. Tadayon*[a] and Z. Sepehri[b]

Received 22nd June 2015
Accepted 27th July 2015

DOI: 10.1039/c5ra12020a

www.rsc.org/advances

A new nanocomposite based on nitrogen-doped graphene nanosheets/$CuCo_2O_4$ nanoparticles was prepared and used as an electrode material for simultaneous determination of dopamine, melatonin and tryptophan. For this purpose, $CuCo_2O_4$ nanoparticles were supported on porous nitrogen-doped graphene nanosheets by a simple method. The nanocomposite was characterized by transmission electron microscopy and X-ray diffraction spectroscopy. Incorporation of the prepared nanocomposite in a carbon paste electrode (CPE) increased the oxidation peak currents and reduced the overpotential of dopamine, melatonin and tryptophan. The new developed sensor was then employed for the simultaneous determination of target analytes with linear ranges of 0.010–3.0 μM, using differential pulse voltammetry. Detection limits of 0.0033, 0.0049 and 0.0041 μM were achieved for dopamine, melatonin and tryptophan, respectively. The selectivity of the method was studied and the results showed that the fabricated sensor is free from interference of organic compounds especially uric acid and ascorbic acid. Finally, the proposed electrochemical sensor was employed to determine analytes in urine, serum and pharmaceutical samples.

Introduction

Over the past decades, to meet the growing demands for ultrasensitive detection, researchers have developed many techniques to enhance the response of electrochemical sensors by modifying them with different functional materials. With the continuous development of nanotechnology, great attention has been paid to different nanomaterials, such as carbon-based nanomaterials, metal nanoparticles (NPs), quantum dots, magnetic NPs and polymeric NPs.[1–4] Because of their biological compatibility, high surface area, chemical stability, excellent catalytic activity and conductivity, the introduction of nanomaterials has really improved the analytical performance of the sensing strategies to obtain amplified detection signals and a stabilized sensing interface with good selectivity.[1–5]

As a two-dimensional single-atom-thick carbon network, graphene (G) has been a research focus due to its unique structure and physiochemical properties.[6] G has exhibited specific characteristics including extremely electric conductivity, large specific surface area, unusual electronic structure, and upstanding thermal conductivity.[6–10] The production of G by the reduction of G oxide (GO) in chemical way produce hydroxyl (–OH) and carboxylate (–COOH) groups in the structure. These active functional groups enable the G structure to interact with metal NPs. These unique properties make G very useful for supporting metal NPs, and the obtained metal-NPs/G nanocomposites exhibit the synergistic effects and good sensitivity in their electrochemical detection behavior.[11,12] The catalytic activity of the metal-NPs upon the electron transfer process paves the way for the production of metal-NPs/G composite based electrochemical sensors.[12,13] However, G sheets tend to irreversible agglomeration and re-stacking because of their strong van der Waals interactions and π–π stacking,[14] which causes some loss of performance for metal-NPs/G nanocomposites in the detection process. Furthermore, low reduction degree (especially for chemically reduced GO) and no-doping properties will also influence their efficiency.[15,16] Thus, the prevention of aggregation and improvement of reduction degree and doping properties are greatly important for reduced graphene oxide (R-GO) in the preparation processes of metal-NPs/G nanocomposites. Nitrogen-doped graphene (N-G) can further improve the reactivity and electrocatalytic performance of G by forming of a delocalized conjugated system with the sp^2-hybridized carbon frameworks ascribed to the lone electron pairs of nitrogen atoms. Moreover, N-G provides abundant binding sites for non-covalent functionalization as well as the enhanced biocompatibility and sensitivity in biosensing applications.[14–17] Also, the N-doping and high reduction degree

[a]*Department of Chemistry, Islamic Azad University, North Tehran Branch, Tehran, Iran. E-mail: f_tadayon@iau-tnb.ac.ir*

[b]*Department of Internal Medicine, Zabol University of Medical Sciences, Zabol, Iran*

properties of N-G as supporter can enhance their own electrical conductivities and improve their own crystal structure, the obtained metal NPs/N-G composites should possess excellent properties for sensing.[14–17]

Among the G based nanocomposite, there are seldom reports about G-spinel cobaltites composite. Complex oxides (containing two or more types of cations) with spinel structure are of intense interests in material research because of their remarkable optical, electrical, magnetic, catalytic properties and widespread applications in science and engineering. Among these, spinel cobaltites (MCo_2O_4, M = Cu, Mn, Ni, Zn, Mg, *etc.*) have recently drawn considerable attention by virtue of their superior physicochemical properties and tremendous potential for many technological applications, ranging from catalysts and sensors to electrode materials and electrochromic devices.[18–20] The combination of N-G with $CuCo_2O_4$ NPs can result in the synergetic effects of two components and exhibit the enhanced performance. The N-G/$CuCo_2O_4$ with rough interface can provide sufficient spaces for the some redox reactions with fast electron transfer rate.

Dopamine (Dp), melatonin (Me) and L-tryptophan (Tp) are important biomolecules that coexist in the extracellular fluid of the central nervous system and serum. These compounds play implicit roles in neurochemistry and biomedicine. Dp is one of the most prominent catecholamines, functioning as a neurotransmitter in the central nervous system. Me, an indoleamine synthesized from an essential amino acid (Tp), is a hormone synthesized by the pineal parenchymal cells from serotonin by N-acetylation and O-methylation and secreted by them into the blood and the cerebrospinal fluid. Dp deficiency and variations in Me levels have been linked to Parkinson's disease. Also, abnormal metabolism of neurotransmitters, particularly DA and ML, is frequently observed in individuals with phenylketonuria and is believed to be involved.[21–23]

Tp is an essential amino acid for humans and a precursor for serotonin, Me and niacin. A significant correlation has been reported between plasma Tp concentrations and depressive illness.[24,25] Recently, effects of Tp and tyrosine supplementation were studied to optimize treatment in phenylketonuria with Dp and Me as biomarkers.[26] Therefore, development of a sensitive and selective method for the determination of Dp, Me and Tp is desirable.

To the best of our knowledge, no study has been published so far reporting the simultaneous determination of Dp, Me and Tp by using any kind of modified electrodes. These species always coexist in biological fluids, and it is very important to develop sensitive and selective sensors for their simultaneous determination of in analytical applications and diagnostic researches. In this work, a simple electrochemical method based on the differential pulse voltammetry (DPV) for the direct determination of Dp, Me and Tp at a N-G/$CuCo_2O_4$/CPE was proposed.

Experimental

Reagents and apparatus

All chemicals and reagents used in this work were of analytical grade and used as received without further purification. Paraffin oil and graphite powder were obtained from Merck Company and used as received. Dp, Me and Tp were prepared from Sigma-Aldrich. Deionized distilled water (DDW) was used to prepare all the solutions. The commercial pharmaceuticals available from a local pharmacy were subjected to the analysis. Britton–Robinson (B–R) solutions were prepared in DDW and were tested as the supporting electrolytes.

Transmission electron microscopic (TEM) images were taken using Zeiss EM902A (Germany). X-ray powder diffraction (XRD, 38066 Riva, d/G.Via M. Misone, 11/D (TN) Italy) was employed to analyze the chemical components of the composites. Electrochemical experiments were carried out at room temperature using a Behpajoh potentiostat/galvanostat system (model BHP-2065). The electrochemical cell was assembled with a conventional three electrode system: a saturated calomel electrode (SCE) as a reference electrode (Azar electrode) and a platinum disk as an auxiliary electrode. Different working electrodes including CPE and modified CPEs were used. The pH measurements were carried out using a Metrohm pH meter (model 713) with a combined pH glass electrode.

Preparation of nanocomposite

Preparation of GO. Natural graphite powder was used to synthesize GO according to a modified Hummers method.[27] Briefly, a mixture of 1 g of graphite and 23 mL of 98% H_2SO_4 was stirred at room temperature over 24 h, and then 100 mg of $NaNO_3$ was added to the mixture and stirred for another 30 min. Subsequently, the mixture was stirred below 5 °C in an ice bath, followed by the slow addition of 3 g of $KMnO_4$ to the graphite powder solution. After vigorous stirring at 35–40 °C for another 30 min, 46 mL of DDW was added to the above mixture. Finally, 140 mL of deionized water and 10 mL of 30% H_2O_2 were introduced into the mixture to complete the oxidation reaction. The GO solution was washed and filtered with HCl. Before complete drying, GO was dispersed in 800 mL of deionized water. The as-synthesized GO was ultrasonically dispersed in anhydrous ethanol for further use.

Preparation of $CuCo_2O_4$ NPs supported on N-RGO. The N-RGO/$CuCo_2O_4$ nanocomposite was prepared by a simple solvothermal method. In a typical synthesis, 1.5 mL of a 0.2 M $Co(OAc)_2$ aqueous solution and 0.75 mL of a 0.2 M $Cu(OAc)_2$ aqueous solution were introduced in to 20 mL of a 0.5 mg mL^{-1} GO ethanolic suspension, followed by the addition of 1 mL of $NH_3 \cdot H_2O$ at room temperature. The reaction was kept at 80 °C in a water bath with stirring for 24 h. After that, the reaction mixture was transferred to a 50 mL teflon-lined autoclave and placed in an oven at 160 °C for 3 h. The resulting product was collected by centrifugation and washed with ethanol and water. For control experimentation, N-RGO was made through the same procedure as N-RGO/$CuCo_2O_4$ except for adding Co and Cu salts. Free $CuCo_2O_4$ NPs were made through the same procedure except for adding GO.[28]

Preparation of the electrodes. The conventional CPE was prepared by hand-mixing of graphite powder and paraffin oil (with a 30/70 paraffin oil/graphite ratio (w/w)) in a mortar and pestle and a portion of the composite mixture was packed firmly

with a piston-driven CPE holder. The G/CPE was prepared by mixing the components of unmodified mixture with G (12%, w/w). The $CuCo_2O_4$/CPE and N-RGO/$CuCo_2O_4$/CPE were prepared by mixing the unmodified mixture with 12% w/w $CuCo_2O_4$ and N-RGO/$CuCo_2O_4$, respectively.

Results and discussion

Characterization of materials

The size, morphology and structure of the resulting materials were investigated by TEM. The morphology of GO, consisting of thin stacked flakes and having a well defined few-layer structure at the edge, can be clearly seen in Fig. 1a. Typical TEM micrograph of $CuCo_2O_4$ (Fig. 1b) shows the formation of uniform and monodispersed $CuCo_2O_4$ NPs with mean diameter and length about 15–25 nm. As shown in Fig. 1c, $CuCo_2O_4$ NPs are grown on a 3D flame like N-RGO and G sheets are completely covered with NPs.

The phase structure of synthesized samples was determined by XRD. The XRD patterns of N-RGO, $CuCo_2O_4$ NPs and N-RGO/$CuCo_2O_4$ are shown in Fig. 1d. The synthesized GO displayed a typical characteristic (002) peak at $2\theta = 10^\circ$.The crystal structure of $CuCo_2O_4$ is in a cubic structure and the fitted lattice parameter of 8.131(5) are in good agreement with the standard JCPDS card no. 78-2177 (a = 8.133 Å). For N-RGO/$CuCo_2O_4$ the diffraction peak arising from GO nearly disappeared at $2\theta = 10^\circ$, suggestive of less agglomeration of the G sheets in the nanocomposite. All of the other diffraction peaks can be indexed to the structure of $CuCo_2O_4$ in nanocomposite.

Electrochemical impedance spectroscopy (EIS)

Fig. 2 exhibits the Nyquist plots of the CPE, G/CPE, $Cu_2Co_2O_4$/CPE and N-RGO/$CuCo_2O_4$/CPE. The CPE (curve a) revealed a very large semicircle domain, implying a very high electron transfer resistance (R_{et}) of the redox probe. After CPE was modified with $Cu_2Co_2O_4$ (curve b) or G (curve c), the R_{et} was a small semicircle domain, showing that the G/CPE and $Cu_2Co_2O_4$/CPE promoted conductivity. When the electrode was conjugated with N-RGO/$CuCo_2O_4$/CPE (curve d), the R_{et} again decreased. This was attributed to that the coating of N-RGO surface with $CuCo_2O_4$ nanoparticles increased the ability of the redox probe to electron transfer. It can be seen that the electron transfer resistance decreased in the order of: bare CPE < $Cu_2Co_2O_4$/CPE < G/CPE < N-RGO/$CuCo_2O_4$/CPE, which

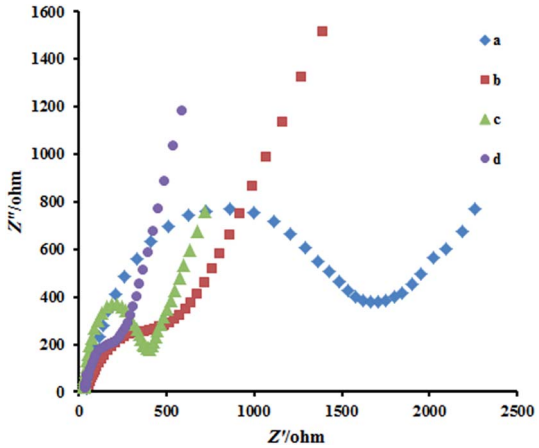

Fig. 2 Nyquist plots for CPE (a) $Cu_2Co_2O_4$/CPE (b) G/CPE (c) N-RGO/$CuCo_2O_4$ (d) in the presence of 1.0 mM $[Fe(CN)_6]^{4-/3-}$ in B–R buffer solution (pH 7.0) with 0.1 M KCl.

implying that $CuCo_2O_4$ and G were excellent electric conducting materials and accelerated the electron transfer.

Electrochemical behavior of analytes

CVs of Dp, Me and Tp at CPE, G/CPE, $CuCo_2O_4$/CPE and N-RGO/$CuCo_2O_4$/CPE in buffer solutions (pH = 3.0) are shown in Fig. 3. At CPE, the peaks of Dp, Me and Tp are rather broad and weak, indicating a slow process of electron transfer (curve b in Fig. 3A–C). For G/CPE and $CuCo_2O_4$/CPE, peaks with defined shape and with the large peak currents were observed (curve c and d). The large oxidation peak current and shift in peak potential to less positive potentials for these electrodes as compared to the CPE indicates the electrocatalytic effect of modified surfaces. Moreover, at N-RGO/$CuCo_2O_4$/CPE, oxidation and reduction peaks of Dp are located at 457 mV and 151 mV showing a smaller peak-to-peak separation than that at CPE. The oxidation peak current is 5.5 times higher than that CPE suggesting the excellent electrocatalytic activity of N-RGO/$CuCo_2O_4$ toward Dp. The similar electrocatalytic activity for Me is also found, which occurs with an increased peak current (5.1 times) and positive shift compared with bare CPE, indicating good electron transfer promotion ability of N-RGO/$CuCo_2O_4$/CPE, also the oxidation peak current of Tp is 9.8 μA,

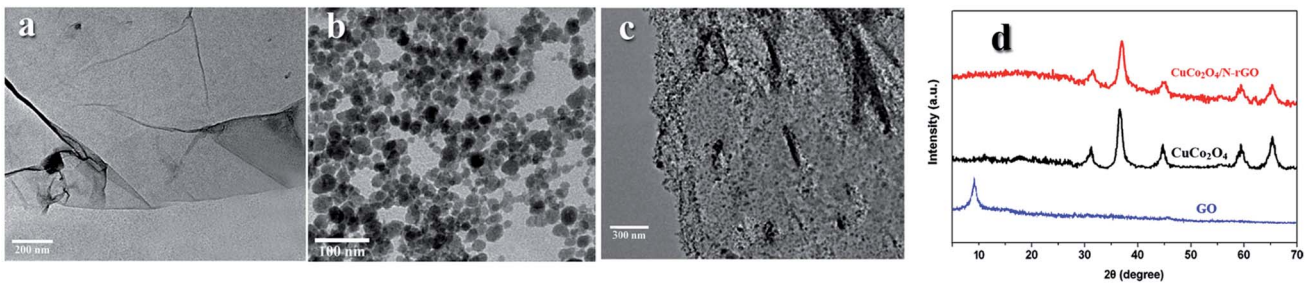

Fig. 1 Comparison of TEM images of (A) GO, (B) $CuCo_2O_4$, (C) $CuCo_2O_4$/N-RGO and (D) XRD patterns.

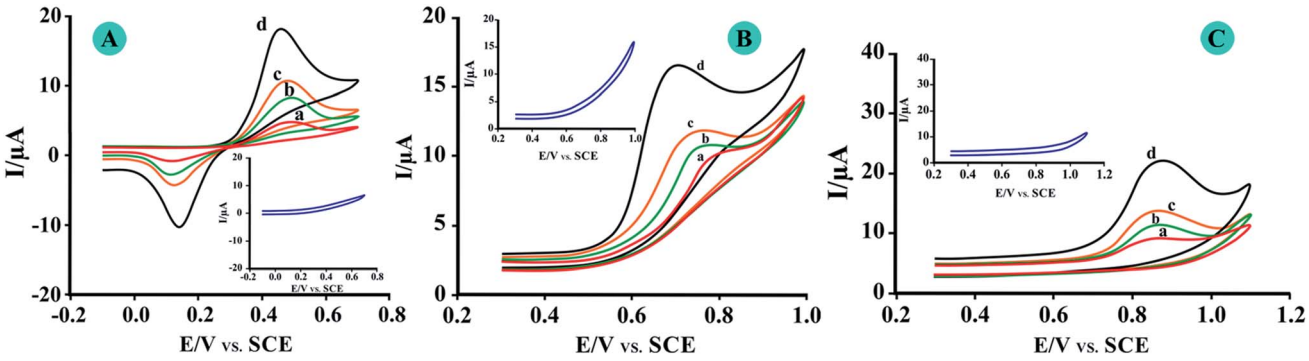

Fig. 3 CVs for (A) 2 μM Dp, (B) 2 μM Me, and (C) 2 μM Tp in B–R buffer solution (pH 3.0) on the surface of various electrodes; curve (a) CPE (b) G/CPE, (c) $CuCo_2O_4$/CPE and (d) $CuCo_2O_4$/N-RGO/CPE in presence of analytes. Insets show $CuCo_2O_4$/N-rGO/CPE in absence of analytes.

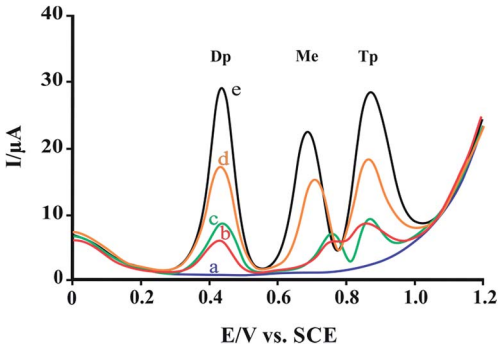

Fig. 4 DPVs of 2 μM Dp, 2 μM Me and 2 μM Tp in B–R buffer solution (pH 3.0) on the surface of various electrodes; curve (a) $CuCo_2O_4$/N-rGO/CPE in absence of analytes, (b) CPE (c) G/CPE, (d) $CuCo_2O_4$/CPE and (e) $CuCo_2O_4$/N-RGO/CPE in presence of analytes.

which is about 5.8 times higher than that at CPE. Insets of Fig. 3 show CVs for N-RGO/$CuCo_2O_4$/CPE in absence of analytes.

Fig. 4 shows the DPV responses at various electrodes in a ternary mixture solution of Dp, Me and Tp with 2.0 μM in B–R buffer solution (pH 3.0). At the CPE only a broad and overlapped oxidation peak is obtained and the potentials of Me and Tp are indistinguishable so that simultaneous determination of these biological molecules is impossible (Fig. 4b). However, at the N-RGO/$CuCo_2O_4$/CPE (Fig. 4e), three sharp and well defined oxidation peaks with larger peak separation potential and higher peak currents corresponding to the oxidation of Dp, Me and Tp were appeared. The three oxidation peaks for Dp, Me and Tp are well resolved at 440, 690 and 840 mV, respectively, with the peak separation potential is 250 mV (Dp–Me) and 150 mV (Me–Tp). All the voltammetric responses can demonstrate that the N-RGO/$CuCo_2O_4$/CPE possess excellent electrocatalytic activities towards the oxidation of Dp, Me and Tp, which can be attributed to its unique structural features and excellent electrochemical properties.[29]

Effect of pH and supporting electrolyte

A series of supporting electrolytes were tested (B–R, phosphate and acetate buffer solutions). Both the peak height and the peak shape were taken into consideration when choosing the supporting electrolyte. Of these, B–R buffer solution gave the best response.

The effect of pH on the response of Dp, Me and Tp evaluated using DPV employing N-RGO/$CuCo_2O_4$/CPE. The effect of pH on peak potential and peak current of Dp, Me and Tp was investigated over the pH range of 2–9 employing B–R buffer solutions. As shown in Fig. 5b, for Dp, with increasing pH, the current increases and reaches a maximum value at pH = 5.0 and decreases with increasing in pH values. The peak currents of Me and Tp initially go up with increasing pH (=3), and then decreases with increasing pH (>3). In addition, Fig. 5c shows that the peak potential of Dp, Me and Tp is also pH dependent and the potentials shifted negatively when the pH of the solutions increases due to the participation of protons in the electrode reaction. The potentials of Dp, Me and Tp followed the linear regression equations with pH: E_{pa} (V) = −0.0602 pH + 0.708 (R = 0.990), E_{pa} (V) = −0.0264 pH + 0.748 (R = 0.984) and E_{pa} (V) = −0.0520 pH + 1.130 (R = 0.992), respectively. For Dp and Tp the slopes is closed to the theoretical value of 59 mV per pH at 25 °C expected from the Nernst equation, indicates that the oxidation process is proton dependent and the electron transfer is accompanied by the transfer of an equal number of protons. Two electrons and two protons are involved for the oxidation of Dp and Tp. In the case of Me, the slope of 0.0264 V pH obtained on N-RGO/$CuCo_2O_4$/CPE was almost similar to that shown in previous electrochemical investigations and it is suggested that the number of electrons transferred in the oxidation of Me is double that of protons.[30,31] The reaction mechanism for the oxidation of Dp, Me and Tp is as given in Scheme 1.

Effect of scan rate on the electrochemical oxidation of Dp, Me and Tp

To investigate the reaction kinetics, the effect of scan rate on the peak currents and peak potentials of Dp, Me an Tp was studied (Fig. 6). Insets of Fig. 6 show that the peak currents changed in a linear relationship with the square root of scan rates in ranges of 10–400, 10–300, and 10–250 mV s^{-1} for Dp, Me and Tp, respectively, and by R-squared values of above 0.99 for all analytes. These plots indicate that the electrochemical reactions for

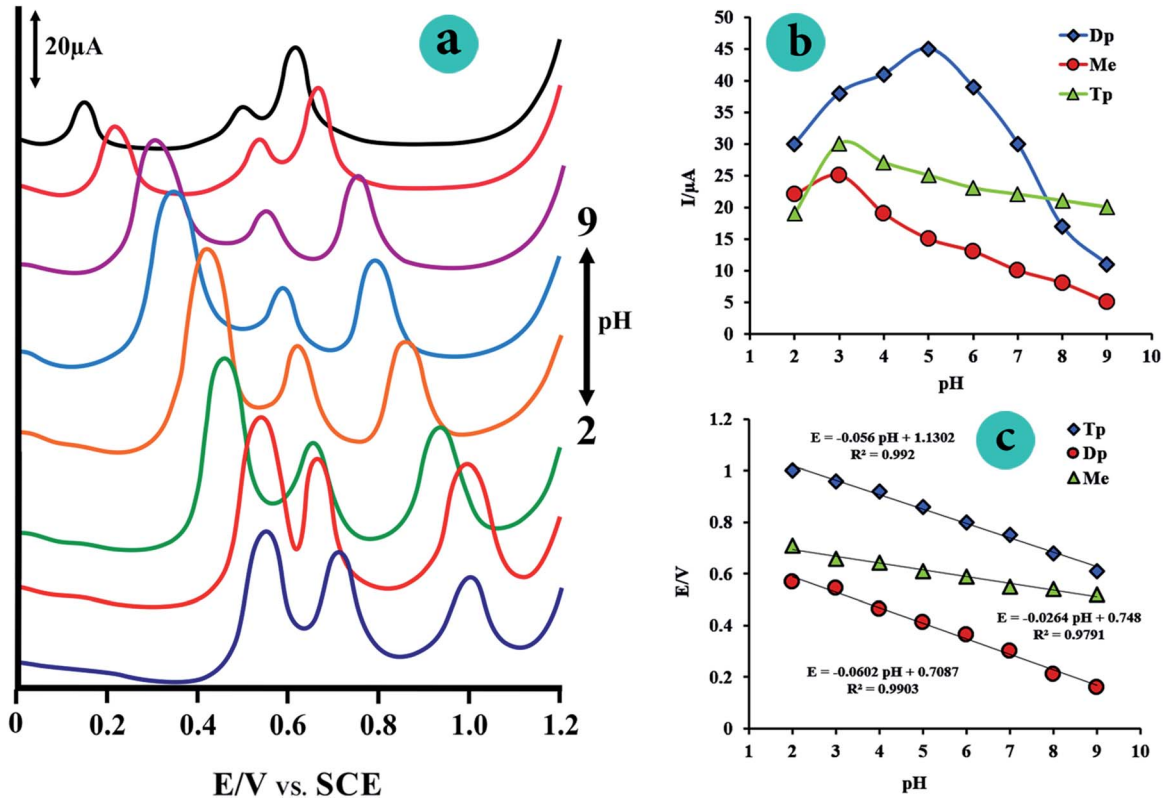

Fig. 5 (a) 3D plots of influence of buffer pH on peak currents and potentials of analyte species, (b) plots of I_p *vs.* pH and (c) plots of E_p *vs.* pH from differential pulse voltammograms of 2.5 μM Dp, Me and Tp in different buffer solution.

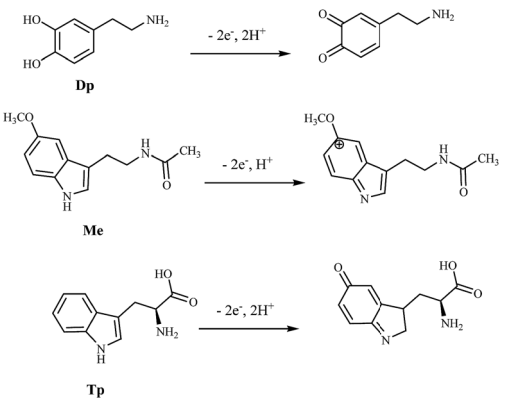

Scheme 1 The oxidation mechanism of Dp, Me and Tp.

these molecules are diffusion controlled. Also for more investigations, log peak currents *versus* log scan rates were plotted for analytes. For these plots when the slope is 0.5, the electrochemical reaction is a diffusion controlled process, and when equals to 1, the electrochemical reaction occurs *via* an adsorption-controlled process.[32] From insets of Fig. 6 the plots of log anodic peak currents *versus* log scan rates have slopes of 0.485, 0.565 and 0.514 for Dp, Me and TP, respectively. These values show that the electrochemical reactions for these biomolecules are governed by diffusion control and the surface of N-RGO/$CuCo_2O_4$/CPE was not fouled by them.

Individual and simultaneous voltammetric determination of Dp, Me and Tp

The above findings enabled us to develop a simple and suitable method for Dp, Me and Tp determination using N-RGO/$CuCo_2O_4$/CPE. As Fig. 7A–C shown, when detecting the individual, the concentration of one substance was changed with the others remained constant. Keeping the concentration of Me and Tp both at 2.0 μM, the peak current increased proportionally with adding concentrations of Dp from 0.010 to 3.0 μM. A linear regression equation between the oxidation peak current with the concentration of Dp was obtained $I_p = 14.98C + 0.4382$ (I_p in μA, C in μM) with $R^2 = 0.9997$. The detection limit for Dp was calculated to be 0.0032 μM. Similarly, to keep the concentration of Dp and Tp both at 2.0 μM, the concentration of Me was changed within the range of 0.010 to 3.0 μM. The linear regression equation of Me was got: $I_p = 10.00C + 0.507$ with $R^2 = 0.9993$. The detection limit for Me was calculated to be 0.0049 μM. In the same way, the concentration of Dp and Me remained were kept at 2.0 μM and the concentration range of Tp was from 0.01 to 3.0 μM, the linear regression equation of Tp was: $I_p = 11.94C + 0.492$ with $R^2 = 0.9907$ and the detection limit for Tp was 0.0041 μM.

The DPVs for different concentrations of Dp, Me and Tp were illustrated in Fig. 8. The resulting calibration plots are linear over the range from 0.01 to 3.0 μM for Dp, Me and Tp. The calibration curves and correlation coefficients are

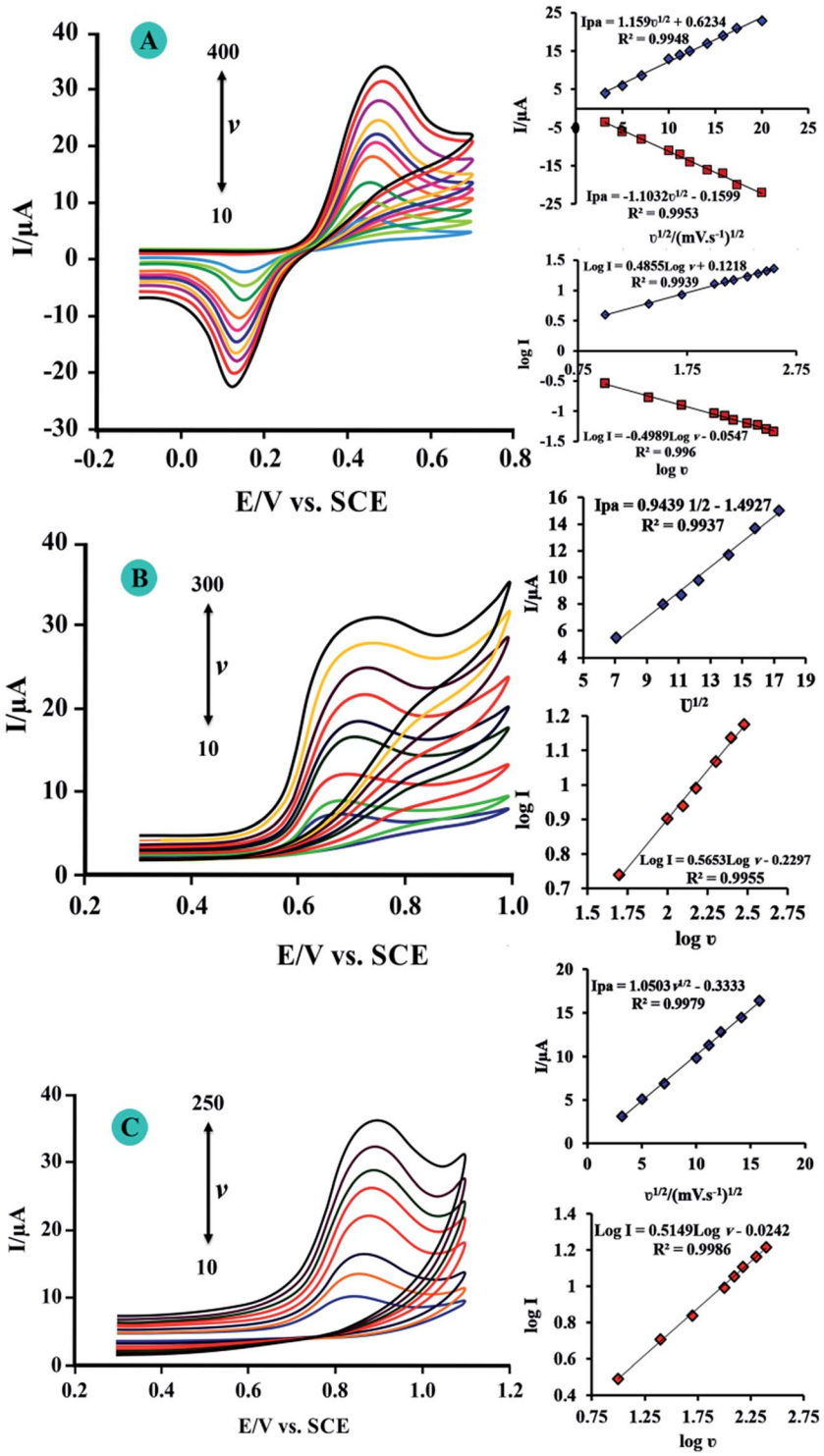

Fig. 6 CVs for $CuCo_2O_4$/N-rGO/CPEin B–R Buffer (pH 3.0) containing 2 μM of (A) Dp with scan rates ranging from a to h as 10–400 mV s^{-1}, respectively (B) Me with scan rates ranging from a to g 10–300 mV s^{-1} and (C) Tp with scan rates ranging from a to f as 10–250 mV s^{-1}. Insets show the linear relationship of the peak current *versus* square root of the scan rate ($\upsilon^{1/2}$) and log peak currents *versus* log scan rate.

$$\text{Dp:}I_p\ (\mu A) = 14.71C_{Dp}\ (\mu M) + 0.521\ R^2 = 0.999$$

$$\text{Me:}I_p\ (\mu A) = 9.95C_{Me}\ (\mu M) + 0.509\ R^2 = 0.997$$

$$\text{Tp:}I_p\ (\mu A) = 11.97C_{Tp}\ (\mu M) + 0.516\ R^2 = 0.998$$

The limits of detection were 0.0033 μM for Dp, 0.0049 μM for Me and 0.0041 μM for Tp based on $3s_b/m$, where s_b is the standard deviation of the mean value for 5 independent voltammetric response of the blank solution.

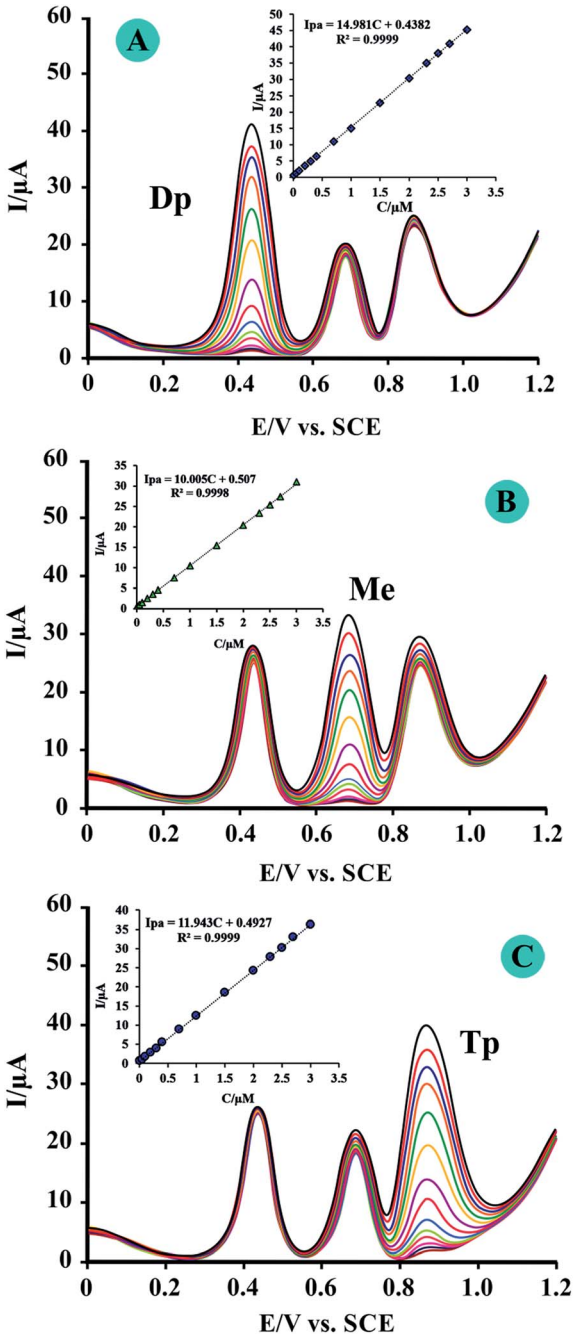

Fig. 7 (A) DPVs for Dp at the $CuCo_2O_4$/N-rGO/CPE in the presence of 2.0 μM Me and Tp in B–R buffer solution (pH = 3.0). Dp concentrations (from a to n): 0.01, 0.05, 0.1, 0.2, 0.3, 0.4, 0.7, 1, 1.5, 2, 2.3, 2.5, 2.7 and 3 μM. (B) DPVs for Me at the $CuCo_2O_4$/N-rGO/CPE in the presence of 2 μM Dp and. Tp concentrations (from a to n): 0.01, 0.05, 0.1, 0.2, 0.3, 0.4, 0.7, 1, 1.5, 2, 2.3, 2.5, 2.7 and 3 μM (C) DPVs for Tp at the $CuCo_2O_4$/N-rGO/CPE in the presence of 2.0 μM Dp and Me in B–R buffer solution (pH = 3.0). Tp concentrations (from a to n): 0.01, 0.05, 0.1, 0.2, 0.3, 0.4, 0.7, 1, 1.5, 2, 2.3, 2.5, 2.7 and 3 μM.

Interferences, stability and reproducibility studies

Several compounds and ions from common co-existing substances were selected to evaluate the anti-interference ability of N-RGO/$CuCo_2O_4$/CPE. The effect of foreign

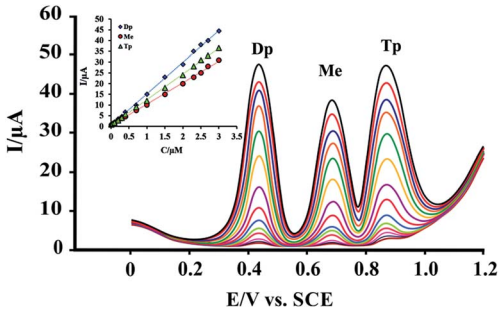

Fig. 8 DPVs for different concentrations of Dp, Me and Tp in pH 3 B–R buffer solution. Concentrations of Dp, Me and Tp from (a) to (n): 0.01, 0.05, 0.1, 0.2, 0.3, 0.4, 0.7, 1, 1.5, 2, 2.3, 2.5, 2.7 and 3 μM.

compounds were tested by analyzing a standard solution of 1.5 μM Dp, 1.0 μM Me and 2.0 μM Tp. The tolerance limit is defined as the maximum concentration of influence substances which causes a ±5% relative error. It is found that species like glucose, lactose and sucrose, uric acid, ascorbic acid (till 100 fold excess), Na^+, K^+, Mg^{2+}, Al^{3+}, CO_3^{2-}, NO_3^-, ClO_4^-, SCN^-(till 1000 fold excess) did not interfere in the analysis of Dp, Me and Tp. The interference caused by same concentration of tyrosine was serious on tryptophan signal. Because tyrosine has similar electroactive group as tryptophan, its oxidation potential is close to tryptophan and thus affect the oxidation peak current of tryptophan. Hence determination of Dp, Me and Tp was not

Table 1 Results for Dp, Me and Tp determination (μM) in various real samples obtained by the proposed method under the optimum conditions

Samples	Analyte	Added (μM)	Found (μM)	Recovery (%)
Urine	Dp	1.00	0.970	97.0
		2.00	2.05	102
	Me	1.00	1.01	101
		2.00	2.06	103
	Tp	1.00	0.980	98.0
		2.00	2.04	102
Human serum	Dp	1.50	1.46	97.3
		2.50	2.45	98.0
	Me	1.50	1.45	96.6
		2.50	2.57	102
	Tp	1.50	1.53	102
		2.50	2.48	99.2
Dp injection	Dp	0.000	0.810	—
		0.500	1.29	97.5
		1.20	2.03	102
	Me	0.500	0.520	104
		1.20	1.24	103
	Tp	0.500	0.480	96.0
		1.20	1.18	98.3
Me tablet	Dp	0.500	0.510	102
		1.20	1.22	102
	Me	0.000	0.540	—
		0.500	1.05	102
		1.20	1.73	98.1
	Tp	0.500	0.510	102
		1.20	1.19	99.1

Table 2 Comparison of some characteristics of the different modified electrodes for the determination of Dp, Me and Tp

Electrode	Method	Linear range (μM)			Detection limit (μM)			Simultaneously with other analytes	Ref.
		ML	DA	TP	ML	DA	TP		
G–Fe_3O_4/CPE	SWV	0.02–5.8	0.02–5.8	—	0.0084	0.0065	—	—	6
ZnO nanorods modified carbon paste electrode	SWV	N.R.	0.3–10.0 and 10.0 to 100.0	—	N.R.	0.056	—	Methionine and caffeine	33
Boron-doped diamond electrode	CV	345–688	—	—	10.3	—	—	—	34
MWNT/GCE	CV	0.08–10	—	—	0.02	—	—	—	35
Boron-doped diamond electrode	SWV	0.5–4	—	—	0.11	—	—	—	27
MWCNTs–CHNPs/CILE	DPV	0.01–50	—	—	0.004	—	—	L-Dopa	36
MnHCFPEDOT/GCE	CV	100–4600	—	—	100	—	—	Catechin	37
TiO_2–GR/4-ABAS/GCE	DPV	—	1–400	1–400	—	0.3	0.3	—	38
GNPs/PImox		—	5.0–268.0	3.0–34.0 and 84.0–464	—	0.08	0.7	Ascorbic acid and uric acid	39
AgNPs/rGO	LSV	—	10–800	10–800	—	5.4	7.5	Ascorbic acid, uric acid	40
GS–PTCA	DPV	—	0.4–370	0.4–140	—	0.13	0.06	Ascorbic acid, uric acid	41
MWCNT/GO	Amperometry	—	—	0.05–4.25	—	—	0.008	—	42
$NiCo_2O_4$/Nano-ZSM-5/GCE	DPV	—	0.6–900	0.9–1000	—	0.5	0.7	Ascorbic acid and uric acid	43
MIP/G	SWV	0.05–100	—	—	0.006	—	—	—	44
N-RGO/$CuCo_2O_4$	DPV	0.01–3.0	0.01–3.0	0.01–3.0	0.0049	0.0033	0.0041	—	This work

considerably affected by common interfering species, which shows that the method is more selective towards the drugs. The stability of the electrode was also tested. The peak current only decreased less than 5% after the electrode was stored at room temperature for 22 days. In addition, in order to evaluate the reproducibility of the modified electrode, a series of five N-RGO/$CuCo_2O_4$/CPEs were prepared for the detection of 2.0 μM of analytes. The RSD ($n = 5$) of peak currents for Dp, Me and Tp were calculated as 3.3%, 3.5% and 3.1%, respectively, which suggests that the reproducibility of the proposed electrode was good. The above results indicate that the as-obtained N-RGO/$CuCo_2O_4$/CPE presents well anti-interference ability, stability and reproducibility.

Determination of Dp, Me and Tp in pharmaceutical, urine and serum samples

To confirm the practical usefulness of this proposed method for simultaneous determination of Dp, Me and Tp in pharmaceutical samples and biological fluids such as human urine, serum, Dp injection and Me tablet were selected as real samples for analysis using the standard addition technique. For sample pretreatments, both urine and serum samples were centrifuged at 5000 rpm for 3 min and the supernatants were collected, finally the prepared samples were diluted 50 times with B–R buffer solution (pH 3.0).

The results are summarized clearly in Table 1, with the recoveries of the spiked samples ranged from 96.0% to 104.0%. It was evident that the N-RGO/$CuCo_2O_4$/CPE could be successfully applied for the simultaneous determination of Dp, Me and Tp in real samples. Moreover, the proposed method has good figures of merits in comparison with other reported methods in literatures. Some figures of merit related to previous reports and the present study are shown in Table 2.

Conclusions

In this work, a novel sensor based on N-RGO/$CuCo_2O_4$ nanocomposite as modifier in CPE, has fabricated that provides an extremely sensitive and selective method for the simultaneous determination of Dp, Me and Tp. Both CV and DPV studies reveal that the potential separations between them were large enough to allow their simultaneous detection. Moreover, appreciable reproducibility and lower detection limits were attained for the three biomolecules at N-RGO/$CuCo_2O_4$/CPE. Hence, it was employed for the analysis of Dp, Me and Tp in human urine, serum and pharmaceutical samples. Recovery values ranging from 97–104% were obtained for real sample analysis. The cost-effectiveness and easy preparative method are added advantages of this sensor. All these factors amalgamate to make this sensor a potential candidate for the detection of these species in routine analysis.

Acknowledgements

The authors gratefully acknowledge the support of this work by the North Tehran Branch, Islamic Azad University.

References

1 C. Zhu, G. Yang, H. Li, D. Du and Y. Lin, *Anal. Chem.*, 2014, **87**, 230–249.
2 A. Walcarius, S. D. Minteer, J. Wang, Y. Lin and A. Merkoçi, *J. Mater. Chem. B*, 2013, **1**, 4878–4908.

3 A. Chen and S. Chatterjee, *Chem. Soc. Rev.*, 2013, **42**, 5425–5438.
4 H. Bagheri, A. Afkhami, Y. Panahi, H. Khoshsafar and A. Shirzadmehr, *Mater. Sci. Eng., C*, 2014, **37**, 264–270.
5 H. Bagheri, R. P. Talemi and A. Afkhami, *RSC Adv.*, 2015, **5**, 58491–58498.
6 A. T. Lawal, *Talanta*, 2015, **131**, 424–443.
7 H. Bagheri, A. Afkhami, P. Hashemi and M. Ghanei, *RSC Adv.*, 2015, **5**, 21659–21669.
8 H. Bagheri, A. Afkhami, H. Khoshsafar, M. Rezaei, S. J. Sabounchei and M. Sarlakifar, *Anal. Chim. Acta*, 2015, **870**, 56–66.
9 A. Afkhami, H. Khoshsafar, H. Bagheri and T. Madrakian, *Sens. Actuators, B*, 2014, **203**, 909–918.
10 A. Afkhami, H. Khoshsafar, H. Bagheri and T. Madrakian, *Anal. Chim. Acta*, 2014, **831**, 50–59.
11 H. Bagheri, S. M. Arab, H. Khoshsafar and A. Afkhami, *New J. Chem.*, 2015, **39**, 3875–3881.
12 E. Er, H. Çelikkan, N. Erk and M. L. Aksu, *Electrochim. Acta*, 2015, **157**, 252–257.
13 S. Pruneanu, F. Pogacean, A. R. Biris, M. Coros, F. Watanabe, E. Dervishi and A. S. Biris, *Electrochim. Acta*, 2013, **89**, 246–252.
14 L. Meng, Y. Xia, W. Liu, L. Zhang, P. Zou and Y. Zhang, *Electrochim. Acta*, 2015, **152**, 330–337.
15 Y. Wang, Y. Shao, D. W. Matson, J. Li and Y. Lin, *ACS Nano*, 2010, **4**, 1790–1798.
16 S. Park, J. An, J. R. Potts, A. Velamakanni, S. Murali and R. S. Ruoff, *Carbon*, 2011, **49**, 3019–3023.
17 H. Xu, J. Xiao, B. Liu, S. Griveau and F. Bedioui, *Biosens. Bioelectron.*, 2015, **66**, 438–444.
18 E. Alizadeh-Gheshlaghi, B. Shaabani, A. Khodayari, Y. Azizian-Kalandaragh and R. Rahimi, *Powder Technol.*, 2012, **217**, 330–339.
19 M. Salavati-Niasari, N. Mir and F. Davar, *J. Phys. Chem. Solids*, 2009, **70**, 847–852.
20 J. Zhu and Q. Gao, *Microporous Mesoporous Mater.*, 2009, **124**, 144–152.
21 D. Bonnefont-Rousselot and F. Collin, *Toxicology*, 2010, **278**, 55–67.
22 T. Meng, Z.-H. Zheng, T.-T. Liu and L. Lin, *Neurochem. Res.*, 2012, **37**, 1050–1056.
23 S. Yano, K. Moseley and C. Azen, *J. Pediatr.*, 2013, **162**, 999–1003.
24 M. Kameya, H. Onaka and Y. Asano, *Anal. Biochem.*, 2013, **438**, 124–132.
25 A. Coppen, E. Eccleston and M. Peet, *The Lancet*, 1972, **300**, 1415–1416.
26 S. Yano, K. Moseley and C. Azen, *J. Pediatr.*, 2014, **165**, 184–189.
27 W. S. Hummers Jr and R. E. Offeman, *J. Am. Chem. Soc.*, 1958, **80**, 1339–1339.
28 R. Ning, J. Tian, A. M. Asiri, A. H. Qusti, A. O. Al-Youbi and X. Sun, *Langmuir*, 2013, **29**, 13146–13151.
29 C. Wei, Q. Huang, S. Hu, H. Zhang, W. Zhang, Z. Wang, M. Zhu, P. Dai and L. Huang, *Electrochim. Acta*, 2014, **149**, 237–244.
30 A. Levent, *Diamond Relat. Mater.*, 2012, **21**, 114–119.
31 W. Xiao-Ping, Z. Lan, L. Wen-Rong, D. Jian-Ping, C. Hong-Qing and C. Guo-Nan, *Electroanalysis*, 2002, **14**, 1654–1660.
32 A. A. Rafati, A. Afraz, A. Hajian and P. Assari, *Microchim. Acta*, 2014, **181**, 1999–2008.
33 E. Molaakbari, A. Mostafavi and H. Beitollahi, *Sens. Actuators, B*, 2015, **208**, 195–203.
34 A. T. Ball and B. A. Patel, *Electrochim. Acta*, 2012, **83**, 196–201.
35 W. Qu, F. Wang, S. Hu and D. Cui, *Microchim. Acta*, 2005, **150**, 109–114.
36 A. Babaei, A. R. Taheri and I. K. Farahani, *Sens. Actuators, B*, 2013, **183**, 265–272.
37 T.-H. Tsai, Y.-C. Huang and S.-M. Chen, *Int. J. Electrochem. Sci.*, 2011, **6**, 3238–3253.
38 C.-X. Xu, K.-J. Huang, Y. Fan, Z.-W. Wu, J. Li and T. Gan, *Mater. Sci. Eng., C*, 2012, **32**, 969–974.
39 C. Wang, R. Yuan, Y. Chai, S. Chen, F. Hu and M. Zhang, *Anal. Chim. Acta*, 2012, **741**, 15–20.
40 B. Kaur, T. Pandiyan, B. Satpati and R. Srivastava, *Colloids Surf., B*, 2013, **111**, 97–106.
41 W. Zhang, Y. Chai, R. Yuan, S. Chen, J. Han and D. Yuan, *Anal. Chim. Acta*, 2012, **756**, 7–12.
42 J. F. Han, Q. Q. Wang, J. F. Zhai, L. Hana and S. J. Dong, *Analyst*, 2015, **140**, 5295–5300.
43 B. Kaur, B. Satpati and R. Srivastava, *New J. Chem.*, 2015, **39**, 1115–1124.
44 P. Gupta and R. N. Goyal, *RSC Adv.*, 2015, **5**, 40444–40454.

